Title

1H detection of heteronuclear dipolar oscillations with water suppression in single crystal peptide and oriented protein samples

Authors

Long, Zheng
Opella, Stanley J

Publication Date

2020-09-01

DOI

10.1016/j.jmr.2020.106793

Peer reviewed

Published in final edited form as:

J Magn Reson. 2020 September ; 318: 106793. doi:10.1016/j.jmr.2020.106793.

^{1}H detection of heteronuclear dipolar oscillations with water suppression in single crystal peptide and oriented protein samples

Zheng Long, **Stanley J. Opella***

Department of Chemistry and Biochemistry, University of California, San Diego, La Jolla, CA 92093-0307, United States

Abstract

Oriented sample solid-state NMR is a complementary approach to protein structure determination with the distinct advantage that it can be applied to supramolecular assemblies, such as viruses and membrane proteins, under near-native conditions, which generally include high levels of hydration as found in living systems. Thus, in order to perform ^{1}H detected versions of multi-dimensional experiments water suppression techniques must be integrated into the pulse sequences. For example, ^{1}H-windowed detection of ^{1}H-^{15}N dipolar couplings enable multi-dimensional NMR experiments to be performed. Here we show that the addition of a solvent suppression pulse during the z-filter interval greatly improves the sensitivity of the experiments by suppressing the ^{1}H signals from water present. This is demonstrated here with a crystal sample submerged in water and then extended to proteins. The combination of solvent-suppressed ^{1}H detected PISEMO and the use of a strip shield-solenoid coil probe configuration provides a two-fold sensitivity enhancement in both the crystal sample and Pf1 coat protein sample compared to the ^{15}N direct detection method. Here we also examine protein NMR line-widths and sensitivity enhancements in the context of window detected separated local field experiments for protein samples.

Keywords

^{1}H detection; Oriented sample solid-state NMR; Protein NMR; Sensitivity enhancement; Single crystal; Strip shield; PISEMO; Water suppression

1. Introduction

Indirect ^{1}H detection is a widely used experimental method in nuclear magnetic resonance (NMR) spectroscopy [1–4]. It provides a number of advantages over conventional approaches to pulsed Fourier-transform NMR spectroscopy, especially sensitivity enhancement.

*Corresponding author. sopella@ucsd.edu (S.J. Opella).

Declaration of Competing Interest

The authors declare that they have no known competing financial interests or personal relationships that could have appeared to influence the work reported in this paper.

Indirect ^{1}H detection was first applied in double-resonance solid-state NMR experiments on organic solids [5], and then in solution NMR [6,7]. Later it was applied to magic angle spinning (MAS) solid-state NMR experiments [8], especially those performed at ultra-fast spinning speeds [9]. In all three cases, static solid-state NMR, solution NMR, and MAS solid-state NMR, sensitivity enhancement was observed in ^{1}H-detected spectra compared to direct-detected spectra only when reasonable ^{1}H resonance line-widths could be obtained [8].

Many methods have been designed that selectively inhibit the strong ^{1}H signals from water in samples of peptides and proteins. One of the most widely used methods is pre-saturation [10]. Compared to other methods taking advantage of the different spin-relaxation time between sample and solvent molecules [11] or using pulsed field gradients (PFG) [12,13], pre-saturation is relatively easy to implement, but can suffer from adverse effects such as the saturation of signals from exchangeable ^{1}H as well as reduction of intensities of signals near the ^{1}H water resonance frequency. However, application of PFG requires additional hardware and more complex pulse sequences.

Moreover, in oriented sample solid-state NMR, the effects of the strong ^{1}H-^{1}H homonuclear dipole-dipole interactions result in large ^{1}H linewidths in the chemical shift dimension [14]. Detection of ^{1}H signals requires both heteronuclear and homonuclear decoupling during signal acquisition which cannot be achieved with conventional continuous acquisition methods of the free induction decay. This is another reason why ^{1}H detection has not seen many applications in oriented sample solid-state NMR.

Windowed detection is an essential aspect of the acquisition of ^{1}H signals. This results in sensitivity enhancement that can be achieved in stationary solid samples such as amorphous proteins [15]. However, the need for resolution among ^{1}H chemical shift frequencies in complex protein spectra limits the wider use of these techniques. Even at high fields, the spans of the ^{1}H chemical shift frequencies are small compared to the resonance line-widths due to the unaveraged dipole-dipole interactions. For example, the ^{1}H line-widths of resonances from partially motionally-averaged residues can be improved to less than 4 ppm in a span of 12 ppm [14]. The less than ideal resolution results in many overlapping signals in one-dimensional spectra of medium and large size proteins. In comparison, the ^{1}H-^{15}N heteronuclear dipolar coupling frequency has a larger span of 10 kHz and relatively narrower resonance line-widths that can be equal to or less than 200 Hz [16]. Therefore, detection of the ^{1}H-^{15}N dipolar coupling frequencies from the amide N-H groups on the protein backbone can provide much better spectral resolution than the detection of the corresponding ^{1}H chemical shift frequencies.

Polarization inversion spin-exchange modulated observation (PISEMO) spectroscopy complements the more widely applied polarization spin-exchange at the magic angle (PISEMA) experiments [17]. The windowed-detection of ^{1}H signals is implemented by directly detecting the oscillating ^{1}H-^{15}N heteronuclear dipolar coupling frequencies [18]. In the PISEMO experiment the ^{1}H channel uses a semi-windowless WaHuHa pulse sequence to attenuate the ^{1}H-^{1}H dipolar interactions. At the same time the matched ^{15}N irradiation induces polarization inversion through spin-exchange under the influence of the

heteronuclear dipolar couplings. This allows the ^{1}H detected PISEMO experiment to directly measure the heteronuclear coupling frequencies in the form of the modulated ^{1}H intensities.

To retain the efficiency of the ^{1}H channel with lossy biological samples, strip shields are often employed to suppress the negative effects of lossy biological samples on the quality factor (Q) of the probe. It was found that when strip shields are incorporated inside a double-tuned solenoid coil, the Q of the high frequency ^{1}H channel is only slightly reduced in the presence of a lossy aqueous sample, without significant attenuation on the Q for the low frequency ^{15}N channel [19]. The application of this coil configuration retains the high filling factors of the ^{1}H channel compared to the cross-coil designs which typically use an orthogonal coil such as the modified Alderman-Grant coil [20] or loop gap resonator [21] for the ^{1}H channel that are larger in size. This probe configuration was chosen to deliver balanced performances for both ^{1}H and ^{15}N detection as well as RF homogeneity [22]. Here we modify the original PISEMO experiment for use with hydrated samples by adding a saturation pulse after cross-polarization and before the multiple pulse sequence on the ^{1}H channel. The model system is a single crystal of N-acetyl leucine (NAL) submerged in water, which allows for testing of the solvent suppression capabilities during the development of the biological sample version of the ^{1}H detected PISEMO pulse sequence. The structural form of the Pf1 coat protein in the filamentous phage particles is chosen as the benchmark protein for ^{1}H detection studies because of its robust stability and ease of magnetic alignment [23] which greatly facilitate experimental optimization. The findings obtained with the relatively simple protein sample can be readily extended to membrane proteins using oriented sample solid-state NMR methods.

2. Experimental methods

The NMR experiments described here involved only two nuclei, ^{1}H and ^{15}N. They were performed on a broad-band spectrometer with a home-built double-resonance probe. The probe's solenoid coil was double-tuned to the ^{1}H (700 MHz) and ^{15}N (71 MHz) resonance frequencies [24]. It incorporated a strip shield in order to minimize the frequency shifts, detuning, and reduction of Q (quality factor) that result from lossy biological samples at high radio-frequencies (RF) [19]. The strip shield consisted of 6 thin (0.05 mm) copper strips (0.8 mm wide × 12 mm long) separated by 0.8 mm on a thin (0.03 mm) Teflon sheet was cut to the appropriate dimensions and rolled into a cylinder that fit within the confines of a 3.2 mm ID solenoid coil made of copper wire with the desired inductance.

Besides the peak tuning frequencies and physical dimensions, the key electrical parameters that determine the performance of the probe are the Q factors of the circuits. The Qs of the ^{1}H and ^{15}N circuits were measured under various conditions using a network analyzer; typical results are shown in Table 1. The Qs of both the ^{1}H and ^{15}N channels were reduced by ~15% upon insertion of a single crystal sample. The Q of the ^{15}N channel with Pf1 bacteriophage and protein-containing bicelle samples were also reduced by ~15%. The effects of placing the strip shield inside the double-tuned solenoid coil are dramatic. Notably, it increased the ^{1}H Q of lossy samples, e.g. the phage sample (~36% increase) and the bicelle sample (~60% increase). This shows that the strip shield plays an essential role in

obtaining spectra with high signal-to-noise ratios with ^{1}H detection methods in solid-state NMR.

The N-acetyl leucine (NAL) crystal was prepared as described previously [24]. 20 μL of water was added to a 4 mg ^{15}N labeled NAL crystal in a 3 mm OD flat bottom glass tube (newera-spectro.com). The bulk of the crystal does not dissolve in water at room temperature. The tube was sealed with a 3 mm OD rubber cap and silicone glue to prevent loss of liquid. The sample arrangement is illustrated in Fig. 1.

Pf1 phage was grown as previously described [23], and then pelleted by centrifugation for four hours at 50k rpm. The pellet was resuspended to a final protein concentration of 50 mg/mL in 20 mM pH 8 borate buffer. 50 μL of sample was placed in a 3 mm × 10 mm glass tube and then sealed as described above. The spectra of the NAL crystal submerged in water were acquired with a power level corresponding to a RF field strength of 55 kHz. The spectra of the Pf1 coat protein were acquired with a power level for a RF field strength of 70 kHz.

The timing diagrams for the pulse sequences are shown in Fig. 2. Both direct and indirect-detect versions of PISEMO without active solvent suppression have been described previously [18]. Timing diagrams for ^{15}N-detected PISEMO and ^{1}H-detected PISEMO are illustrated in Fig. 2A and 2B, respectively. In applications of ^{1}H-detected PISEMO to the NAL crystal in water, the experimental parameters used to obtain the results in Fig. 3 were: 2 scans, 128 t_1 points, and 4 s z-filter. The large signal from the solvent (water) was suppressed by applying continuous wave RF irradiation of 7 kHz magnitude at the precise resonance frequency of the ^{1}H water signal during the z-filter interval. Optimization of the irradiation consisting of minimizing both the magnitude of the applied RF power as well as the duration of the irradiation used as the saturation pulse during the z-filter. Saturation pulses with X, Y, X, and Y phases were applied in the ^{1}H-detected PISEMO experiment illustrated with the results shown in Fig. 4B, E and F. Each of the four 1 s RF pulses generated a 10 kHz B_1 field.

The ^{15}N detected PISEMO spectra were acquired with a 55 kHz field strength, 4 scans and 256 t_1 points. The ^{1}H detected PISEMO spectra were acquired with a 55 kHz field strength, 2 scans and 512 t_1 points. The spectra of solvent-free crystals shown in Fig. 5B and D were acquired with 4 scans and 256 t_1 points with a 53 kHz field strength. Each of the X, Y, X, Y-phase saturation pulses were 0.2 s long in order to match the pulse durations used in the protein experiments. The power levels were either 12 kHz or 0 kHz in order to determine whether there is any signal attenuation due to the saturation irradiation. The magnitude of the irradiation was selected based on the optimized values used for the protein sample. The NMR spectra of the single crystal samples were acquired at room temperature.

^{1T5}N-detected PISEMO spectra of Pf1 bacteriophage in aqueous solution were acquired with 64 scans and 128 t_1 points (1.73 ms scaled acquisition time). The ^{1}H-detected PISEMO spectra of Pf1 bacteriophage were acquired with 32 scans and 256 t_1 points (5.12 ms). These spectral parameters enabled both dimensions of the spectra to have the same acquisition times. In the ^{1}H-detected experiments, a total of four 12.5 kHz field strength 0.2 s long

pulses with phases X, Y, X, and Y were used. These parameters were optimized to minimize both the magnitude of the irradiation and the z-filter duration. The NMR spectra of Pf1 phage coat protein were acquired at 0 °C. The dwell time for the ^{15}N detection experiment in t_2 was 40 μs, and the dwell time for the ^{1}H detection experiment in t_2 was 0.1 μs; each dwell contains a pair of complex points.

Data processing was performed using the program Topspin 3.1 (www.bruker.com) with the python module. Data points were taken from the selected detection windows. The data were phase shifted to maximize the signal intensity of the real data, then real data points were selected from the distorted points in the beginning and end of the detection window, and subsequently compiled into a complete data set. The data points from the same detection window were summed. In the presented experimental data, samples were taken at 0.05 μs intervals. In each detection window, 1.4 μs of data was extracted, which corresponds to 28 complex points, of which 14 are real points. Imaginary points were discarded. Sine bell squared functions were applied to the protein data: in the two-dimensional experimental data, a 45° shift for the chemical shift dimension and a 60° shift for the dipolar coupling frequency dimension resulted in spectra with optimal peak shapes. No shaped or line-broadening functions were applied to the one-dimensional spectral slices in order to preserve the veracity of the intensities used to compare signal-to-noise ratios. Resonance assignments were based on previously published results [23].

3. Results and discussion

Each of the four molecules in the unit cell of NAL have a distinctive orientation. Consequently, a solid-state NMR spectrum of a NAL has four signals, each of which is characterized by a unique frequency along the chemical shift and dipolar coupling axes. This accounts for the resolution among signals in the spectra presented in Figs. 3–5. As a result, differences of crystal orientations produce different resonance frequencies in the one- and two-dimensional spectra.

The ^{15}N chemical shift and ^{1}H-^{15}N dipolar coupling frequencies are readily measured for each amide site in two-dimensional separated local field (SLF) spectra of single crystals of ^{15}N labeled NAL. High resolution spectra result from the implementation of WHH-4 for homonuclear decoupling. In order to perform ^{1}H detected PISEMO on proteins in aqueous solution it is necessary to add water suppression to the pulse sequences.

In ^{1}H detected PISEMO experiments the ^{1}H - ^{15}N heteronuclear dipolar coupling frequencies are observed directly. Most solvent molecules and phospholipids do not have ^{15}N-^{1}H bonds. In addition, because ^{1}H chemical shift frequencies are not directly measured, solvent signals, in theory, would not interfere with protein signals. However, residual solvent signals are still strong and have to be dealt with to obtain spectra with high sensitivity. Noise from solvent signals is not completely random; this is seen between ±4 kHz in Fig. 3A with a NAL single crystal sample submerged in water. Because the spectrum in Fig. 3A was collected without solvent suppression, the signal and noise have similar intensities as manifested by their having similar contour levels.

Application of low power continuous wave irradiation during the z-filter interval greatly reduces the unwanted noise. This is illustrated by the experimental data shown in Fig. 3B. Comparing the resonances in the contour plot in Fig. 3A to those in Fig. 3B enables the signals from the NAL single crystal to be readily distinguished from the noise in Fig. 3A. Comparison of the one-dimensional slices in Fig. 3C and D show that the signal-to-noise ratio is substantially improved by the implementation of water suppression on aqueous samples. This is the main justification for the present development. Because of the limited dynamic range of pre-amplifiers and intermediate frequency amplifiers as well as nonlinear behavior of mixers and other components in heterodyne receivers, the reduction in intensity of strong signal(s), i.e. from water, is crucial for recording weak signals i.e. from proteins, without excessive distortion.

In Fig. 3B, a 4 s saturation pulse was required to sufficiently suppress the water signals using 7 kHz power, by contrast in Fig. 3A where the 4 s pulse was replaced with a 4 s delay the signals are overwhelmed by noise. In addition to the CW method, application of the 90° phase shifts during the saturation pulse was attempted. This phase shift was developed to destroy unrelated ^{1}H t_1 noise [25]. It is shown in Fig. 4 that the 4 phase-shifted pulses can replace the CW saturation pulse for the water submerged crystal sample. The total duration of the saturation was 4 s at a 10 kHz power level. In this experiment, a two-fold enhancement of the signal-to-noise ratio was obtained when compared to the ^{15}N detected spectrum, as shown in comparisons of the signal-to-noise levels in the slices in Fig. 4C and D versus those in Fig. 4E and F. Seconds-long durations of the saturation pulses cannot be used on proteins because they typically have local and global motions that greatly reduce T_1. This renders the CW method unfavorable for application to proteins, since it requires long saturation intervals to be effective.

When four phase-shifted pulses are applied during the time interval the z-filter of the PISEMO experiment, the time required for saturation of the magnetization can be reduced, shortening the overall experimental time. For example, for the Pf1 coat protein sample, the z-filter interval can be as short as 0.8 s. This is significant for the application of the method to protein samples, where the amide ^{15}N T_1 is on the order of 10 s. To demonstrate that saturation during the z-filter does not affect the NMR signals, the ^{1}H detected PISEMO experiment was performed on a dry NAL single crystal with and without the saturation pulses. The results are shown in Fig. 5 where comparison of Fig. 5A (with) and B (without) the application of the saturation pulses yield nearly identical spectra. The intensities of the resonance signals in the spectral slices shown in Fig. 5C and D are very similar down to the same noise level. It may be possible to further improve solvent suppression by taking advantage of a homospoil z-gradient as incorporated into the MAS experiment MISSISSIPI [26] or a gradient coil with available accessories. Sufficient suppression of large solvent signals results in the ^{1}H detected PISEMO spectrum of Pf1 coat protein shown in Fig. 6B.

Two-dimensional spectra of the structural form of Pf1 coat protein in virus particles were acquired using ^{15}N-detected PISEMO (Fig. 6A) and ^{1}H-detected PISEMO with solvent suppression (Fig. 6B). With equivalent data processing the resulting spectra are very similar. They are also similar to the previously published PISEMO spectra [23].

Thiriot et al. [23] observed all 40 of the amide resonance signals expected at 0 °C in the helical region of the spectrum. Here 38 resonances are observed in the same spectral region. The two weakest signals reflect a smaller amount of sample in the coil and reduced signal averaging. All of the line widths are similar; ~250 Hz in the chemical shift dimension and ~500 Hz in the heteronuclear dipolar coupling dimension.

To make comparisons of the sensitivities of the ^{1}H-detected PISEMO spectra with the ^{15}N-detected PISEMO spectra, the number of scans in the ^{15}N detected experiments are doubled. The indirect dimension of the ^{15}N-detected PISEMO experiment measures phase-insensitive ^{1}H-^{15}N dipolar coupling frequencies while the indirect dimension of the ^{1}H-detected PISEMO experiment measures phase-sensitive ^{15}N chemical shift frequencies. Indirect measurement of chemical shift generally requires two 90° phase-shifted acquisitions for each t_1 value. The signal enhancement factors have been demonstrated previously [8,14,17]:

$$\xi = (0.177)(\gamma_H/\gamma_N)^{3/2}(W_N/W_H)^{1/2}(Q_H/Q_N)^{1/2}(\eta_H/\eta_N)(SW_H/FW_H)^{1/2} \quad (1)$$

Eq. (1) can be used to determine the sensitivity enhancement factor ξ. The gyromagnetic ratio factor $(\gamma_H/\gamma_N)^{3/2}$ is 31.6 for ^{1}H-^{15}N heteronuclear experiments. The probe quality factor ratio $(Q_H/Q_N)^{1/2}$ is 1.73 as calculated from measured values given in Table 1. The sample filling factor ratio η_H/η_N is 1 for a single coil probe design. Thus, Eq. (1) reduces to:

$$\xi = (9.68)(W_N/W_H)^{1/2}(SW_H/FW_H)^{1/2} \quad (2)$$

The term $(SW_H/FW_H)^{1/2}$ influences the sensitivity enhancement factor because a much larger filter bandwidth (FW) has to be used compared to the spectral width (SW) [15]. In our experiments, in order to sample as fast as possible, we used a filter width of 200 MHz for a one-dimensional 10 MHz spectral width. In comparison, the ^{15}N-detected experiments used a 125 kHz filter bandwidth and 25 kHz spectral width. This larger filter width allowed more ^{1}H noise into the ^{1}H-detected data, reducing the signal/noise ratio. This is reflected in the $(SW_H/FW_H)^{1/2}$ factor which equals 0.224. In practice, this can be more accurately calculated by counting the data points in the detection windows due to our data processing method [18].

Throughout most of the detection window, the receiver gate was blocked, and no signal or noise was allowed through. During the detection windows, the effective dwell time is then equivalent to the multiple pulse cycle time. Distorted points within the detection window due to digital filtering are removed during data processing. The removal of the distorted points reduced the effective filter width to $1/t_{s,}$ where t_s is the duration span of the total amount of the usable data within each detection window. In the protein experiment, 1.4 μs of usable signal data points in each cycle of 27 μs results in a $(SW_H/FW_H)^{1/2}$ value of 0.228. This value is different from previously calculated 0.224 because it reflects the removal of the distorted data points. In data processing, a total of 14 real data points was summed which resulted in 1.83 times enhancement compared to the case without such processing in the protein sample. As a result, combined with the previous calculations, 4.04 times signal enhancement for a peak that has $W_N = W_H$ can theoretically be achieved.

$$\xi = (4.04)(W_N/W_H)^{1/2} \quad (3)$$

In our protein sample, we observed a range of resonance line widths. The symbols W_N and W_H represent the resonance line widths for the directly detected dimensions: W_N for ^{15}N detected experiments and W_H for ^1H detected experiments. Various levels of sensitivity enhancements for different residues were found within the same sample. Typical resonances have a ^{15}N chemical shift linewidth of 200 Hz, and a ^1H - ^{15}N dipolar coupling frequency linewidth of 600 Hz. This results in a theoretical sensitivity enhancement factor of 2.33. This is close to what is observed in our experimental data shown in Fig. 6. For example, the one-dimensional slices taken for the signal from I39 in the ^1H detected experiments (Fig. 6E) have 1.84 (Fig. 6E) fold sensitivity enhancement for the ^{15}N chemical shift dimension compared to ^{15}N detection (Fig. 6C). For the ^1H - ^{15}N dipolar coupling frequency dimension (Fig. 6C), a 2.10-fold enhancement of the signal-to-noise ratio was obtained compared to ^{15}N detection (Fig. 6D). The application of the 0.8 s saturation pulse during z-filter also contributes to some loss of sensitivity during the ^1H detection pulse due to T_1 relaxation. This effect is estimated to be less than 10% based on the magnitude of the protein ^1H T_1.

Based on this analysis, the ^1H - ^{15}N heteronuclear dipolar coupling frequency linewidth is the limiting factor in the sensitivity of the ^1H-detected PISEMO spectra. To improve the performance of the ^1H window-detection experiments, better multiple pulse sequences need to be implemented to improve ^1H - ^1H dipole-dipole averaging. The Pf1 coat protein spectra were acquired at 0 °C but when larger amplitude molecular motions in samples such as bilayer samples under physiological temperatures, protein linewidths are narrower. The averaging due to rotational diffusion affects the decay of the ^1H-^{15}N dipolar coupling and ^{15}N chemical shift induction decay by different amounts. In recent studies, the resonance linewidths of Pf1 coat protein in aligned triton bicelles can be improved to as narrow as 90 Hz for their ^{15}N chemical shift, and to 150 Hz for their ^1H-^{15}N dipolar coupling frequency at physiological temperatures and a ^1H frequency of 900 MHz [24]. Further line-width improvements can be obtained with the use of aligned macrodiscs [27]. These bilayer samples are in sharp contrast to the phage bound Pf1 coat protein used in this study which demonstrates broader line-widths and at a much lower temperature of 0 °C which quenches molecular motions. Therefore, it is likely that more fully optimized membrane protein samples can receive additional benefits from the ^1H-detected PISEMO technique. Another factor which limits the sensitivity enhancements is the use of the States method [28] for phase sensitive ^{15}N chemical shifts detection in the indirection dimension. It requires two separate acquisitions for each t_1 value, which doubles the overall experimental time. Many methods have been developed to shorten the acquisition requirements for the indirect dimensions. In particular, non-uniform sampling with data reconstruction [29–32] are becoming more widely employed in protein NMR spectroscopy. These and other methods have the potential to further improve water-suppressed versions of ^1H detected two-dimensional solid-state NMR experiments.

4. Conclusions

^{1}H-detected one- and two-dimensional heteronuclear NMR experiments on stationary peptide and protein samples can be improved by incorporation of RF pulses that suppress the strong signals from water. Here water suppression was successfully accomplished in PISEMO experiments on aligned samples of Pf1 coat protein in its structural form in phage particles and in its membrane-bound form in phospholipid bilayers. The inclusion of solvent signal suppression during the z filter enabled ^{1}H-detected PISEMO experiments to be performed on protein samples in aqueous solution, which resulted in the first two-dimensional spectra of aligned proteins to be obtained with windowed detection. The sensitivity enhancement from the use of ^{1}H detection is around two-fold compared to direct ^{15}N detection when applied to the Pf1 phage coat protein samples. The indirect detection approach for NMR of stationary samples remains at an early stage of development especially. Especially since the levels of signal enhancement varies for proteins with different ^{15}N resonance linewidths and dipolar coupling frequency linewidths. This method is particularly well suited for future studies of membrane proteins that are oriented in the magnetic field.

Acknowledgements

We thank Dr. Chin Wu for assistance with instrumentation and data processing, Dr. Jinfa Ying for assistance with data processing, and Dr. Sabrina Berkamp and Dr. Jasmina Radoicic for assistance with sample preparation. This research was supported by grants P41EB002031 and R35GM122501 from the National Institutes of Health and utilized the Biomedical Technology Resource Center for NMR Molecular Imaging of Proteins at the University of California, San Diego.

References

[1]. Andreas LB, Jaudzems K, Stanek J, Lalli D, Bertarello A, Le Marchand T, Paepe DCD, Kotelovica S, Akopjana I, Knott B, Wegner S, Engelke F, Lesage A, Emsley L, Tars K, Herrmann T, Pintacuda G, Structure of fully protonated proteins by proton-detected magic-angle spinning NMR, P. Natl. Acad. Sci. USA 113 (2016) 9187–9192.

[2]. Bax A, Subramanian S, Sensitivity-enhanced two-dimensional heteronuclear shift correlation Nmr-spectroscopy, J. Magn. Reson 67 (1986) 565–569.

[3]. Live DH, Davis DG, Agosta WC, Cowburn D, Observation of 1000-fold enhancement of N-15 Nmr via proton-detected multiquantum coherences - studies of large peptides, J. Am. Chem. Soc 106 (1984) 6104–6105.

[4]. Muller L, Sensitivity enhanced detection of weak nuclei using heteronuclear multiple quantum coherence, J. Am. Chem. Soc 101 (1979) 4481–4484.

[5]. Grannell PK, Mansfield P, Whitaker MA, C-13 double-resonance Fourier-transform spectroscopy in solids, Phys. Rev. B 8 (1973) 4149–4163.

[6]. Bax A, Griffey RH, Hawkins BL, Sensitivity-enhanced correlation of N-15 and H-1 chemical-shifts in natural-abundance samples via multiple quantum coherence, J. Am. Chem. Soc 105 (1983) 7188–7190.

[7]. Bodenhausen G, Ruben DJ, Natural abundance N-15 Nmr by enhanced heteronuclear spectroscopy, Chem. Phys. Lett 69 (1980) 185–189.

[8]. Ishii Y, Tycko R, Sensitivity enhancement in solid state N-15 NMR by indirect detection with high-speed magic angle spinning, J. Magn. Reson 142 (2000) 199–204. [PubMed: 10617453]

[9]. Lewandowski JR, Dumez JN, Akbey U, Lange S, Emsley L, Oschkinat H, Enhanced resolution and coherence lifetimes in the solid-state NMR spectroscopy of perdeuterated proteins under ultrafast magic-angle spinning, J. Phys. Chem. Lett 2 (2011) 2205–2211.

[10]. Hoult DI, Solvent peak saturation with single-phase and quadrature Fourier transformation, J. Magn. Reson 21 (1976) 337–347.

[11]. Patt SL, Sykes BD, Water eliminated Fourier-transform Nmr-spectroscopy, J. Chem. Phys 56 (1972) 3182–3184.

[12]. Chevelkov V, van Rossum BJ, Castellani F, Rehbein K, Diehl A, Hohwy M, Steuernagel S, Engelke F, Oschkinat H, Reif B, 1H detection in MAS solid-state NMR spectroscopy of biomacromolecules employing pulsed field gradients for residual solvent suppression, J. Am. Chem. Soc 125 (2003) 7788–7789. [PubMed: 12822982]

[13]. Hurd RE, Gradient-enhanced spectroscopy, J. Magn. Reson 213 (1990) 467–473.

[14]. Lu GJ, Park SH, Opella SJ, Improved H-1 amide resonance line narrowing in oriented sample solid-state NMR of membrane proteins in phospholipid bilayers, J. Magn. Reson 220 (2012) 54–61. [PubMed: 22683581]

[15]. Hong M, Yamaguchi S, Sensitivity-enhanced static 15N NMR of solids by 1h indirect detection, J. Magn. Reson 150 (2001) 43–48. [PubMed: 11330982]

[16]. Nevzorov AA, Opella SJ, Selective averaging for high-resolution solid-state NMR spectroscopy of aligned samples, J. Magn. Reson 185 (2007) 59–70. [PubMed: 17074522]

[17]. Wu CH, Ramamoorthy A, Opella SJ, High-resolution heteronuclear dipolar solid-state Nmr-spectroscopy, J. Magn. Reson., Ser A 109 (1994) 270–272.

[18]. Wu CH, Opella SJ, Proton-detected separated local field spectroscopy, J. Magn. Reson 190 (2008) 165–170. [PubMed: 17981481]

[19]. Wu CH, Grant CV, Cook GA, Park SH, Opella SJ, A strip-shield improves the efficiency of a solenoid coil in probes for high-field solid-state NMR of lossy biological samples, J. Magn. Reson 200 (2009) 74–80. [PubMed: 19559634]

[20]. Grant CV, Yang Y, Glibowicka M, Wu CH, Park SH, Deber CM, Opella SJ, A Modified Alderman-Grant Coil makes possible an efficient cross-coil probe for high field solid-state NMR of lossy biological samples, J. Magn. Reson 201 (2009) 87–92. [PubMed: 19733108]

[21]. Gor'kov PL, Chekmenev EY, Li C, Cotten M, Buffy JJ, Traaseth NJ, Veglia G, Brey WW, Using low-E resonators to reduce RF heating in biological samples for static solid-state NMR up to 900 MHz, J. Magn. Reson 185 (2007) 77–93. [PubMed: 17174130]

[22]. Grant CV, Wu CH, Opella SJ, Probes for high field solid-state NMR of lossy biological samples, J. Magn. Reson 204 (2010) 180–188. [PubMed: 20435493]

[23]. Thiriot DS, Nevzorov AA, Opella SJ, Structural basis of the temperature transition of Pf1 bacteriophage, Protein Sci. 14 (2005) 1064–1070. [PubMed: 15741342]

[24]. Long Z, Park SH, Opella SJ, Effects of deuteration on solid-state NMR spectra of single peptide crystals and oriented protein samples, J. Magn. Reson 309 (2019) 106613. [PubMed: 31677452]

[25]. Ishii Y, Yesinowski JP, Tycko R, Sensitivity enhancement in solid-state C-13 NMR of synthetic polymers and biopolymers by H-1 NMR detection with high-speed magic angle spinning, J. Am. Chem. Soc 123 (2001) 2921–2922. [PubMed: 11456995]

[26]. Zhou DH, Rienstra CM, High-performance solvent suppression for proton detected solid-state NMR, J. Magn. Reson 192 (2008) 167–172. [PubMed: 18276175]

[27]. Radoicic J, Park SH, Opella SJ, Macrodiscs comprising SMALPs for oriented sample solid-state NMR spectroscopy of membrane proteins, Biophys. J 115 (2018) 22–25. [PubMed: 29914645]

[28]. States DJ, Haberkorn RA, Ruben DJ, A two-dimensional nuclear overhauser experiment with pure absorption phase in 4 quadrants, J. Magn. Reson 48 (1982) 286–292.

[29]. Barna JCJ, Laue ED, Mayger MR, Skilling J, Worrall SJP, Exponential sampling, an alternative method for sampling in two-dimensional Nmr experiments, J. Magn. Reson 73 (1987) 69–77.

[30]. Hoch JC, Modern spectrum analysis in nuclear magnetic resonance: alternatives to the Fourier transform, Methods Enzymol. 176 (1989) 216–241. [PubMed: 2811688]

[31]. Rovnyak D, Frueh DP, Sastry M, Sun ZY, Stern AS, Hoch JC, Wagner G, Accelerated acquisition of high resolution triple-resonance spectra using non-uniform sampling and maximum entropy reconstruction, J. Magn. Reson 170 (2004) 15–21. [PubMed: 15324754]

[32]. Ying J, Delaglio F, Torchia DA, Bax A, Sparse multidimensional iterative lineshape-enhanced (SMILE) reconstruction of both non-uniformly sampled and conventional NMR data, J. Biomol. NMR 68 (2017) 101–118. [PubMed: 27866371]

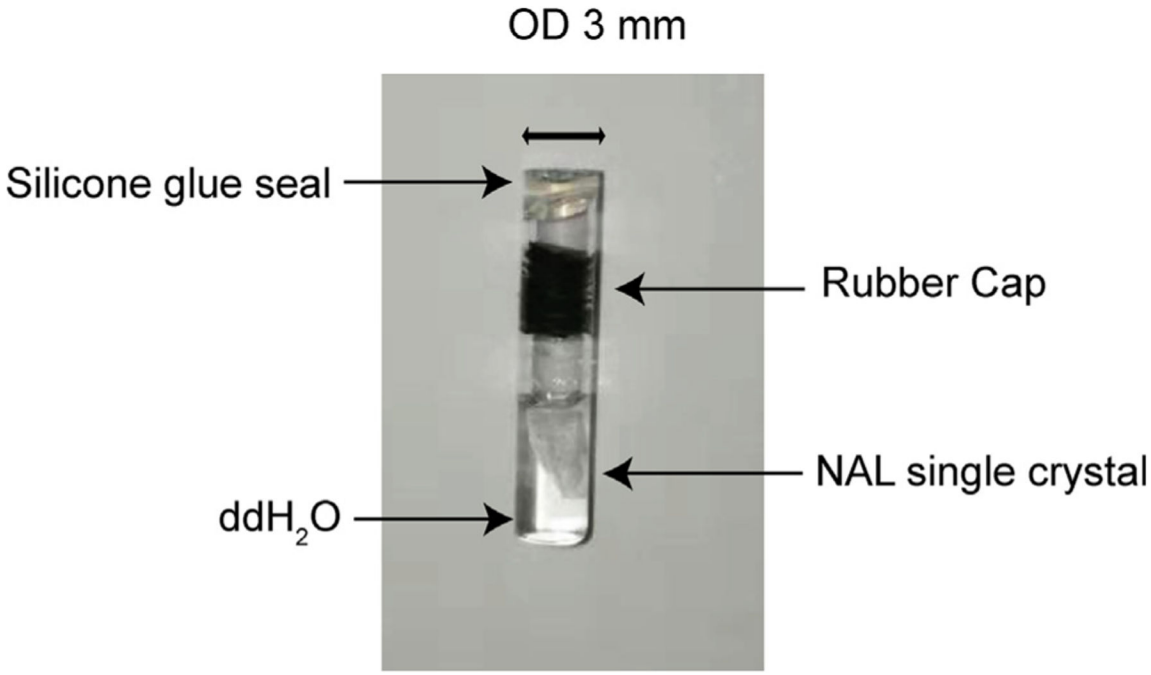

Fig. 1.

Picture of the water submerged single crystal sample placed in a 3 mm OD flat bottom NMR tube, capped with a piece of black rubber, and sealed with silicone glue to prevent losing of liquid due to evaporation. Double distilled (dd) water was used as in biological samples.

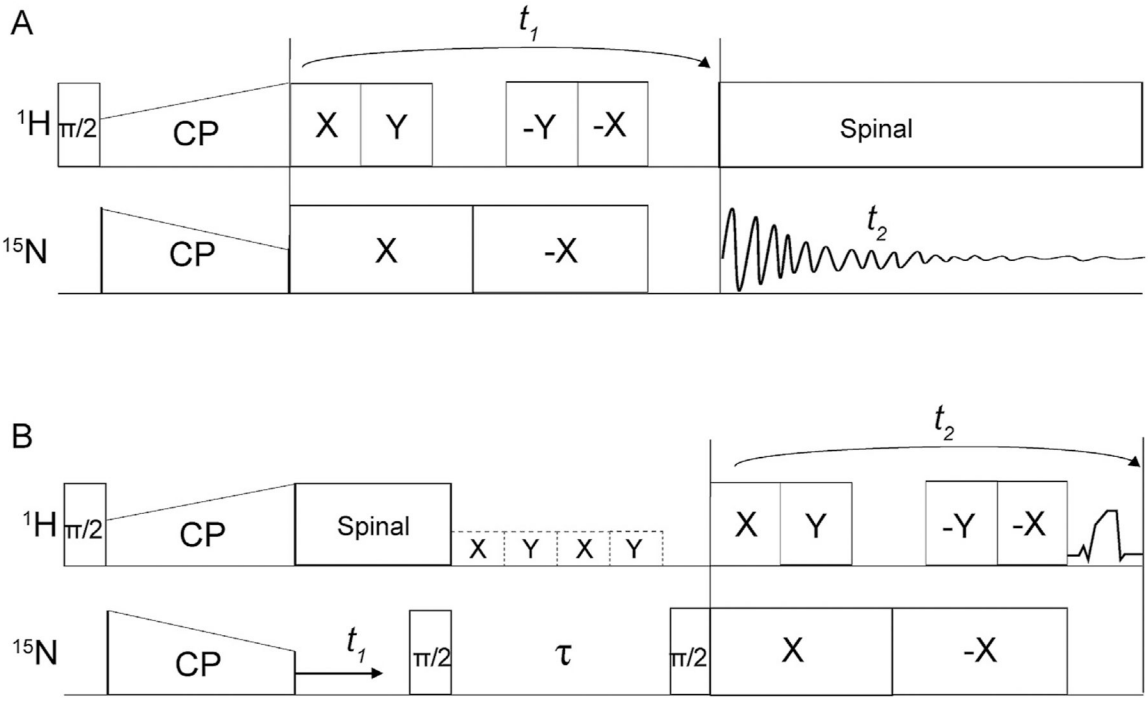

Fig. 2.

Timing diagrams for the pulse sequences used in the ^{1}H- and ^{15}N-detected PISEMO experiments. (A) ^{15}N-detected PISEMO. (B) ^{1}H-detected PISEMO. Dashed boxes indicate the saturation pulses applied during the z-filter to effect water suppresion. The pulses consist of 4 blocks of 0.2 s 13 kHz pulses with the phases in the order of X, Y, X, Y. (A-B) cross polarization utilizes double ramps with 60%−100% amplitudes amplitudes on the ^{1}H channel and 100%−60% amplitudes on the ^{15}N channel; both have a duration of 1 ms. During the multiple pulse cycles, the 4 pulses on the ^{1}H channel have phases in the order of X, Y, −Y, −X for the odd number cycles, and −X, −Y, Y, X for the even number cycles. The two pulses on the ^{15}N channel have phase X and −X for odd number cycles, and −X and X for even number cycles.

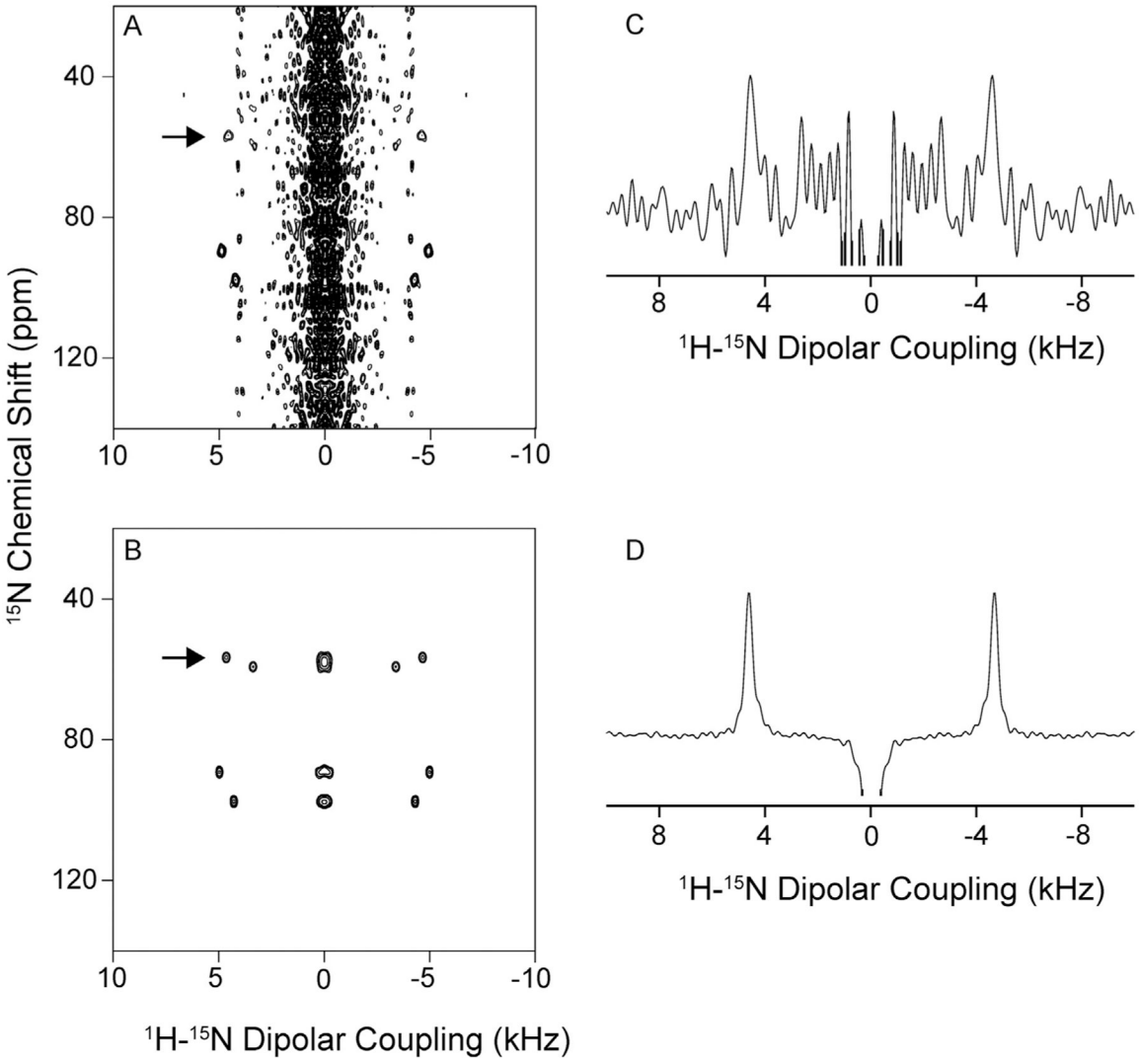

Fig. 3.

A ^{15}N labeled NAL crystal submerged in water was used to demonstrate the water suppression method. Spectra were acquired with 2 scans, 128 t_1 points and 55 kHz field strength. (A) and (B) are two-dimensional ^{1}H detected PISEMO spectra shown with the full dipolar coupling frequency span. (A) With a 4 s delay without irradiation during the z-filter. (B) With a 7 kHz continuous wave saturation pulse during the 4 s z-filter. (C) and (D) are one-dimensional slices through the frequency marked by the arrow in (A) and (B), respectively.

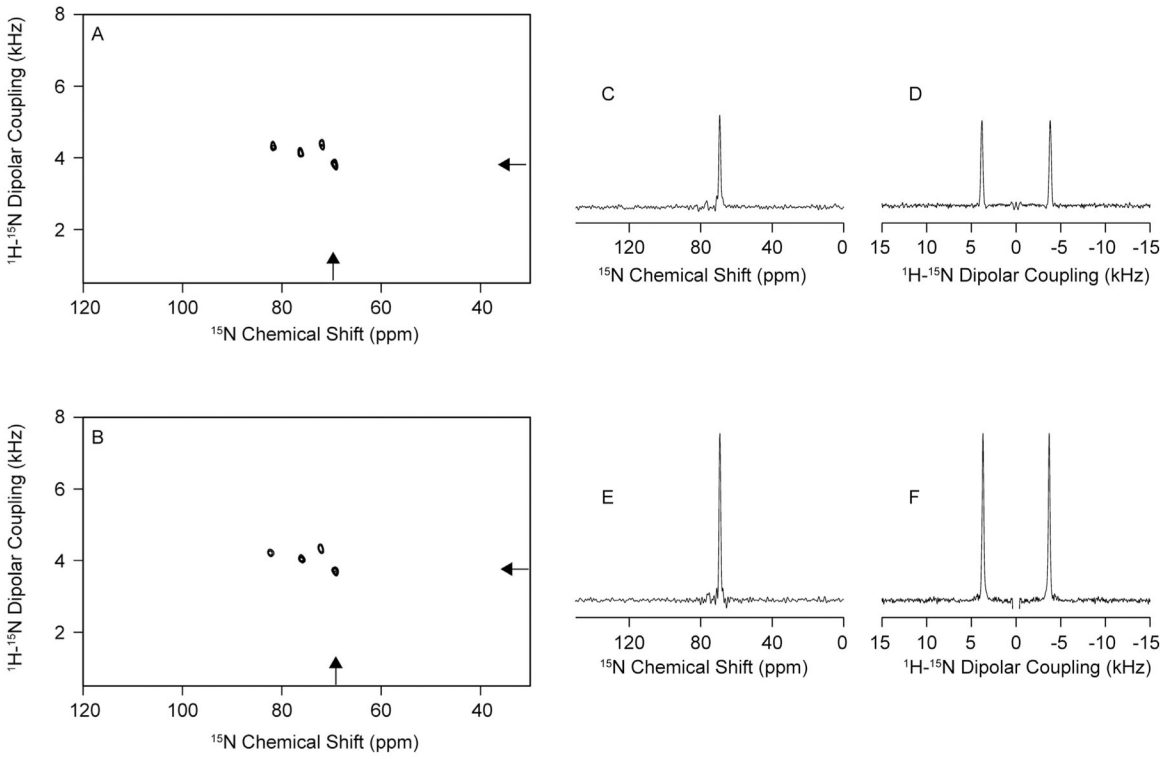

Fig. 4.

A ^{15}N labeled NAL crystal submerged in water was used to demonstrate the water saturation method. (A) is the ^{15}N detected PISEMO spectrum acquired with 4 scans and 256t points and 55 kHz field strength. (B) is the ^{1}H detected PISEMO spectrum acquired with 2 scans, 512 t_1 points and 55 kHz. Four 10 kHz 1 s long water suppression pulses of phases X, Y, X, Y were applied during the 4 s z-filter. (C) and (E) are ^{15}N chemical shift dimension slices at the frequency marked by the arrow in (A) and (B) respectively. (D) and (F) are ^{1}H-^{15}N dipolar coupling frequency dimension slices at the frequencies marked by the arrow in (A) and (B) respectively.

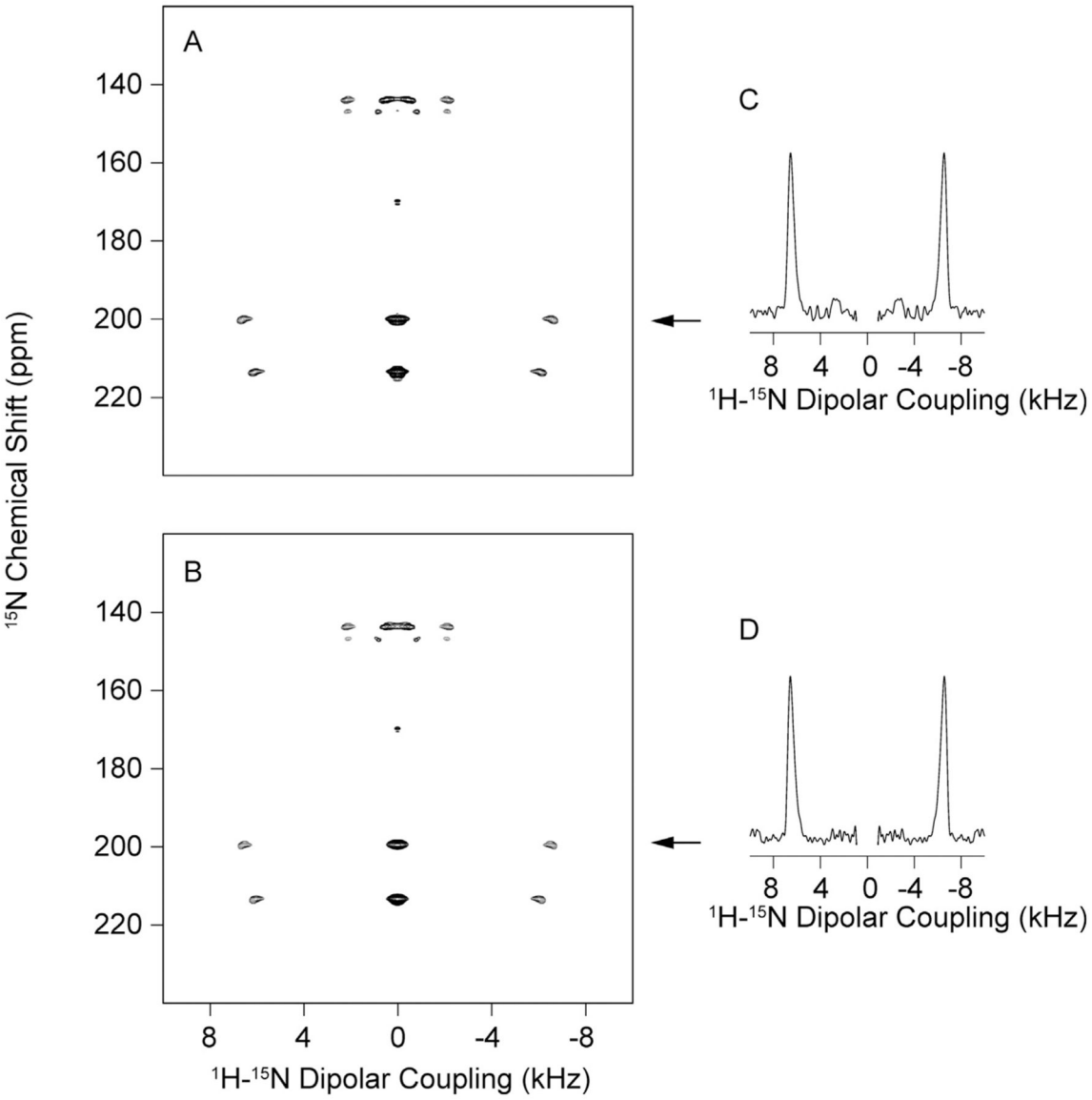

Fig. 5.

A ^{15}N labeled NAL crystal was used to demonstrate that the water saturation method does not suppress ^{1}H signals from NAL. (A) and (B) are two-dimensional ^{1}H detected PISEMO spectra acquired with 4 scans, and 256 t_1 points with a 53 kHz field strength. (A) Four 12.5 kHz field strength 1 s long water suppression pulses with phases X, Y, X, Y were applied during the z-filter. (B) No power was applied during a 0.8 s z-filter. (C) and (D) are ^{1}H-^{15}N dipolar coupling frequency dimension slices at the frequencies marked by marked by the arrows in (A) and (B) respectively.

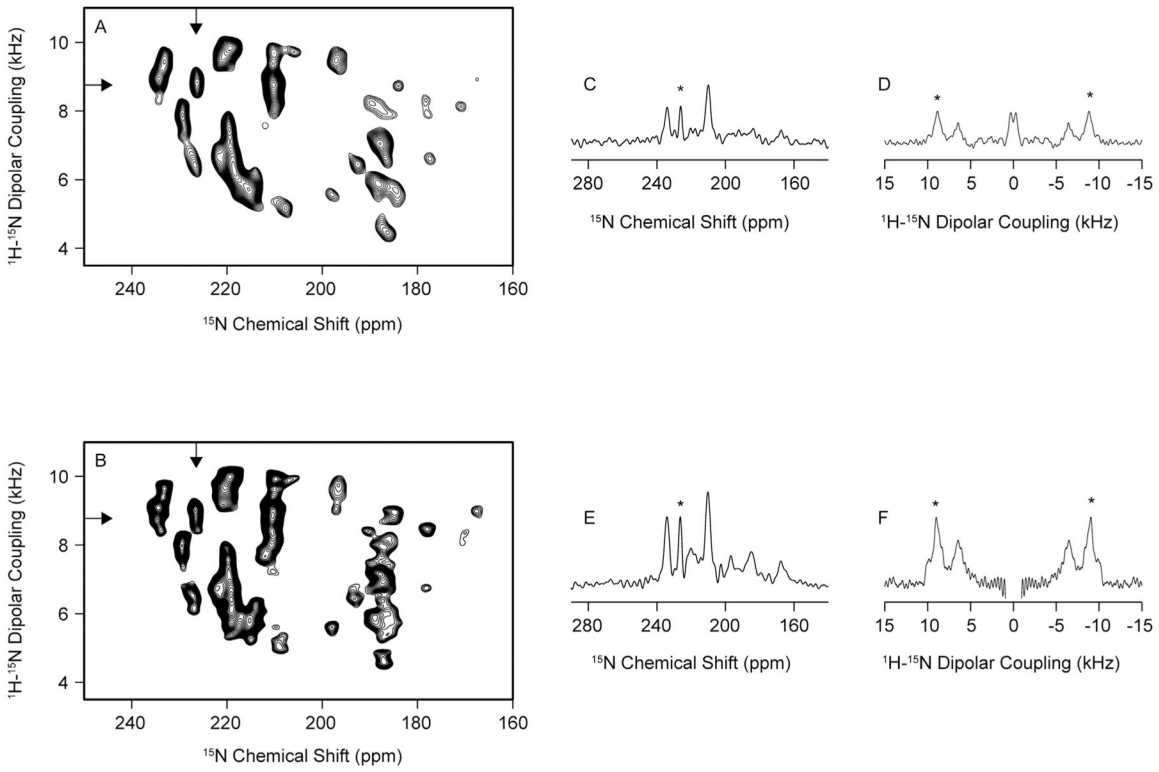

Fig. 6.

Comparisons of the PISEMO spectra of Pf1 coat protein in phage and their one-dimensional slices. (A) ^{15}N detected PISEMO spectrum acquired at 70 kHz with 64 scans and 128 t_1 points. (B) ^{1}H detected PISEMO spectrum acquired at 70 kHz with 32 scans and 256 t_1 points. (C and D) are one dimensional ^{15}N chemical shift and ^{1}H-^{15}N dipolar frequency slices through the signal from I39 taken from (A). (E and F) are one dimensional ^{15}N chemical shift and ^{1}H-^{15}N dipolar frequency slices through the signal from I39 taken from (B). The arrows points to the frequencies where the slices are taken, and the asterisk in (C–F) identify the location of the I39 signals in the spectra.

Table 1

Quality factor of the 1H and 15N RF channels with and without a strip-shield for various samples.

	^{1}H Channel (only solenoid)	^{15}N Channel (only solenoid)	^{1}H Channel (with stripshield)	^{15}N Channel (with stripshield)
Single peptide crystal	186	59	155	50
Pf1 phage in solution	110	60	150	50
Protein-containing bicelle	86	57	138	50